Supplemental Methods

Experimental IBD models, ^{18}F-FSPG PET imaging, and *ex vivo* analysis

Two experimental IBD models, induced by DSS in male Balb/c mice, aged 8–9 weeks and weighing 20–25g (Central Lab Animal, Inc., Seoul, Republic of Korea), and adoptive transfer of naïve T cells ($CD4^+CD45RB^{high}$) into male immunodeficient RAG2-knockout (BALB/c-$Rag2^{-/-}\gamma c^{-/-}$) mice, aged 8–12 weeks and weighing 25–35 g (Jackson Laboratory, Bar Harbor, ME, USA), were evaluated. The experimental unit was an individual animal, independently and nonrandomly allocated to a colitis or control group. Analysis of sample size showed that the minimum number of animals in each colitis or control group was 5 to 8, based on a significance level of $P < 0.05$ and a power of 80% for various differences in ^{18}F-FSPG uptake between IBD and control groups with a 15% or 20% coefficient of variation. Animals in the experimental IBD models were included in this study if they showed symptoms or signs of inflammation. Animals were excluded if they had lost >20% body weight during the study. These criteria were defined before the experiment. Researchers were aware of the group allocation during the conduct of the experiment and the assessment of clinical outcomes.

To induce colitis with dextran sulfate sodium (DSS), mice were administered 5% DSS (MP Biomedicals, Solon, OH, USA) in drinking water ad libitum for 7 days, followed by administration of normal drinking water. Body weight, rectal bleeding, and diarrhea were monitored daily. Clinical disease activity was determined as the average of weight loss scores (0, none; 1, 1–5%; 2, 5–10%; 3, 10–20%; 4, >20%), stool consistency scores (0, normal; 2, loose; 4, diarrhea), and bleeding scores (0, absence; 2, hematocrit positive; 4, gross bleeding).

To induce colitis by transfer of T cells, $CD4^+$ T cells were isolated from the spleens of wild-type BALB/c mice and purified using a $CD4^+$ T-cell isolation kit (Miltenyi Biotech, Bergisch

Gladbach, Germany), followed by staining with anti-CD4 (RM4-5) and anti-CD45RB (16A) antibodies (BD Biosciences, Franklin Lakes, NJ, USA). $CD4^+CD45RB^{high}$ T-cells were sorted on a FACS Aria sorter (BD Biosciences). BALB/c background $Rag2^{-/-}\gamma c^{-/-}$ mice were injected i.p. with 5×10^5 $CD4^+CD45RB^{high}$ T cells. Body weight and diarrhea were monitored twice weekly. Clinical disease activity was determined as the average scores for weight loss (0, none; 2, 5–15%; 4, >15%) and stool consistency (0, normal; 2, mild symptoms; 4, severe diarrhea).

Mice were subjected to ^{18}F-FSPG PET imaging 1 week after DSS administration and 8–12 weeks after adoptive T-cell transfer using an animal PET/magnetic resonance imaging (PET/MRI) system (nanoScan PET/MRI, MEDISO, Ltd., Hungary). Static PET images were acquired 60 minutes after injection of 7.4 MBq (0.2 mCi) into the tail vein for 10 minutes. The standardized uptake value (SUV) was calculated using the formula: SUV = (tissue radioactivity in the volume of interest measured as MBq/cc × body weight) / injected radioactivity. The maximum value (SUVmax) in each mouse was chosen for analysis.

Immediately after PET imaging, the mice were sacrificed and the colon removed. The entire colon of each mouse was cut lengthwise and washed with phosphate-buffered saline, fixed in 4% paraformaldehyde, embedded in paraffin, and stained with Hematoxylin-Eosin. Pathologic scoring was performed in a blinded fashion. Mice with DSS-induced colitis were scored using a system based on three parameters: severity of inflammation (0, none; 1, slight; 2, moderate; 3, severe), extent of injury (0, none; 1, mucosa; 2, mucosa and submucosa; 3, transmural and loss of epithelium), and crypt damage (0, none; 1, basal one-third damaged; 2, basal two-thirds damaged; 3, only surface epithelium intact; 4, entire crypt and epithelium lost). The sum of the three scores was multiplied by a factor that reflected the percentage of tissue involvement (1, 0–25%; 2, 26–50%, 3, 51–75%; 4, 76–100%). Mice with IBD induced by T-cell transfer were subjected to

pathologic scoring based on crypt architecture (0, normal; 1, irregular; 2, moderate crypt loss (10–50%); 3, severe crypt loss (50–90%); 4, small/medium sized ulcers (<10 crypt widths); 5, large ulcers (>10 crypt widths); crypt abscesses (0, normal; 1, 1–5; 2, 6–10; 3, >10); tissue damage (0, normal; 1, discrete lesions; 2, mucosal erosions; 3, extensive mucosal damage); inflammatory cell infiltration (0, occasional; 1, increased leukocytes in the lamina propria; 2, confluence of leukocytes extending to the submucosa; 3, transmural extension of inflammatory infiltrates); and goblet cell loss (0, normal to <10% loss; 1, 10–25% loss; 2, 25–50% loss; 3, >50% loss). The total pathological score was calculated by combining scores of the five parameters, with a maximum score of 17.

Immunohistochemical staining of mouse colon

Colon tissues were obtained from three mice each with DSS-induced and T-cell transfer-induced colitis and three corresponding control mice each, fixed in 4% paraformaldehyde and dehydrated in 15% and 30% sucrose solutions in phosphate-buffered saline. Tissues were embedded in optimal cutting temperature compound, and sections were fixed with acetone at -20°C for 5 minutes. Slides were blocked by incubation in phosphate-buffered saline (PBS) containing 1% bovine serum albumin for 1 hour at room temperature and stained with primary antibodies against x_C^-, glucose transporter, and cell surface markers overnight at 4°C. After washing in PBS, the tissue samples were incubated with secondary antibodies at room temperature for 1 hour and stained with 4′,6-diamidino-2-phenylindole (Thermo, Waltham, MA, USA) for 2 minutes at room temperature, followed by mounting with PermaFluor mountant (Thermo). Images were captured on an LSM 710 confocal microscope (Carl Zeiss, Oberkochen, Germany). The primary antibodies were Alexa Fluor 488-conjugated anti-glucose transporter GLUT1 (EPR3915), rabbit anti-xCT (polyclonal),

hamster anti-CD11c (HL3), PE-conjugated anti-CD3 (17A2), and PE-conjugated anti-F4/80 (CI:A3-1). Secondary antibodies were Alexa Fluor 568-conjugated goat anti-hamster IgG and Alexa Fluor 647 donkey anti-rabbit IgG. Antibodies were purchased from BD Biosciences, BioLegend (San Diego, CA, USA), Abcam (Cambridge, UK), and Novus Biologicals (Littleton, CO, USA).

Clinical study: Criteria for inclusion and exclusion

Inclusion criteria

A subject will be enrolled if s/he meets all of the following inclusion criteria:

- Subject is aged between 19 and 79 years, is male or female, and is of any race/ethnicity.
- Subject has had UC or CD diagnosed by clinical, endoscopic, and histologic evidence for at least 3 months prior to screening.
- Subject has symptoms suggestive of active disease at the time of enrollment.
- Subject is scheduled to undergo sigmoidoscopy or colonoscopy for UC or CD within 7 days prior to or after the planned ^{18}F-FSPG administration.

Exclusion criteria

A subject is to be excluded from the study if s/he does not fulfill all of the inclusion criteria or displays any of the following exclusion criteria:

- Subject or his/her legally acceptable representative does not provide written informed consent.

- Subject displays clinical signs of ischemic colitis or has evidence of pathogenic bowel infection.
- Subject has been diagnosed as having unclassified inflammatory bowel disease.
- Subject has been treated with sulfasalazine or intravenous corticosteroids within the previous 4 weeks prior to the planned ^{18}F-FSPG administration.
- Dose escalation of current IBD drugs or start of a new oral aminosalicylate, corticosteroid, immunomodulator, biologics, antibiotics, probiotics, or topical preparations is scheduled from the time of study enrollment to the scheduled sigmoidoscopy or colonoscopy, or 24 hours after ^{18}F-FSPG administration. Dose escalation or starting a new antidiarrheal and/or analgesic drug is allowed.
- Female subject is pregnant or nursing. The possibility of pregnancy is excluded if 1) a woman is physiologically post-menopausal (cessation of menses for more than 2 years); 2) a woman is surgically sterile (has had a documented bilateral oophorectomy and/or documented hysterectomy; or 3) a woman of childbearing potential is negative on a serum or urine pregnancy test performed within 24 hours immediately prior to administration of ^{18}F-FSPG; the latter women are advised to utilize contraceptive measures during participation in this study.
- Subject has concurrent severe and/or uncontrolled and/or unstable medical disease (e.g., congestive heart failure, acute myocardial infarction, severe pulmonary disease, chronic renal or hepatic disease) that, in the opinion of the investigator, could compromise participation in the study.
- Subject is a relative or student of the investigator, or is otherwise dependent on the investigator.

- Subject has received any investigational drugs or devices within 4 weeks prior to study enrollment.
- Subject was previously included in this study.
- Subject has any other condition or personal circumstances that might make a collection of complete data difficult or impossible, in the judgment of the investigator.
- Subject is allergic to hyoscine or any of the ingredients of hyoscine butylbromide, or has myasthenia gravis, megacolon, closed-angle glaucoma, or obstructive prostatic hypertrophy.

^{18}F-FSPG PET/CT imaging of patients: safety and interpretation

The safety of ^{18}F-FSPG was assessed based on laboratory parameters (serum chemistry), vital functions (blood pressure, heart rate, and body temperature), and physical examinations at baseline and 3 hours after ^{18}F-FSPG injection. Follow-up safety information was collected again at 24 hours. Adverse events were continuously monitored from patient enrollment until the last ^{18}F-FSPG-related adverse events were resolved, or up to a maximum of 28 days after the follow-up visit.

Based on the knowledge of ^{18}F-FSPG biodistribution (*1,2*), the intensity of ^{18}F-FSPG uptake was classified according to a 5-point scale, with 1 indicating no uptake above background; 2 indicating uptake less than or equal to a blood pool; 3 indicating uptake greater than the blood pool but less than or equal to that of the liver; 4 indicating moderately higher uptake compared with the liver; and 5 indicating markedly increased uptake compared with the liver. The location and intensity of ^{18}F-FSPG activity were assessed in the rectum, sigmoid colon, descending colon, transverse colon, and ascending colon of patients with UC; and in the rectum, sigmoid and descending colon, transverse colon, ascending colon, and ileum of patients with CD. The maximum ^{18}F-FSPG score was the highest value among segmental scores, with a score ≥4 considered positive for active disease. In our retrospective analysis approved by the institutional review board of Asan Medical Center (2019-0052), only 4 (2.2%) of 180 bowel segments from the subjects with no history of IBD had scores ≥4 (*1,2*). For quantitative analysis, volumes of interest were drawn on each bowel segment, using the combined CT data for anatomical localization.

Assessment of clinical and pathological assessment of disease activity

Clinical disease activity was assessed in patients with UC using the partial Mayo score, and patients with CD using the Crohn's Disease Activity Index and Harvey-Bradshaw Index (*3*). Bowel segments were histologically evaluated by an experienced pathologist, who was blinded to the results of ^{18}F-FSPG PET/CT, using the Robarts Histopathological Index for patients with UC (*3*) and the Colonic and Ileal Global Histological Disease Activity Score for patients with CD, with the latter modified by excluding the number of biopsies.

Immunohistochemical staining of human xCT, GLUT1, and cell surface markers

Multiplex immunofluorescence staining was performed using a Leica Bond Rx™ Automated Stainer (Leica Biosystems, Newcastle, U.K), as described previously (*4*). Tissue sections were incubated with primary antibodies, followed by a secondary polymer-horseradish peroxidase-bound antibody (Polymer HRP MS + Rb, ARH1001EA; Akoya Biosciences, Marlborough, MA, USA). Images of multiplex immunofluorescence staining were captured using the Vectra Polaris Automated Quantitative Pathology Imaging System (Akoya Biosciences). A region of interest was placed on the abnormal mucosa that revealed abnormal features of inflammatory bowel disease, as determined by an experienced pathologist. Immune cell populations positive for xCT, GLUT1, and cell surface markers were characterized and quantified by tissue segmentation, cell segmentation, and phenotyping, as determined by inForm version 2.2 software (Akoya Biosciences). Batch analysis was performed on each tissue's selected region of interest using the same algorithm designed for representative images. The number of cells with each phenotype was

calculated using RStudio version 1.3.1073 software and classified using TIBCO Spotfire™ (TIBCO Software, Palo Alto, CA, USA). The numbers of labeled cells per mm^2 were quantified.

Statistical analysis

Continuous variables are reported as median and range, whereas categorical variables are reported as numbers (%). Quantitative variables were compared by Mann–Whitney U-tests. Associations between variables were assessed by nonparametric Spearman rank correlation coefficient analysis. The inter-reader variability of visual assessment of ^{18}F-FSPG accumulation was assessed using kappa statistics with 95% confidence intervals. All statistical analyses were conducted using IBM SPSS Statistics for Windows (version 21; IBM Company, Armonk, NY), with two-sided *P*-values <0.05 considered statistically significant.

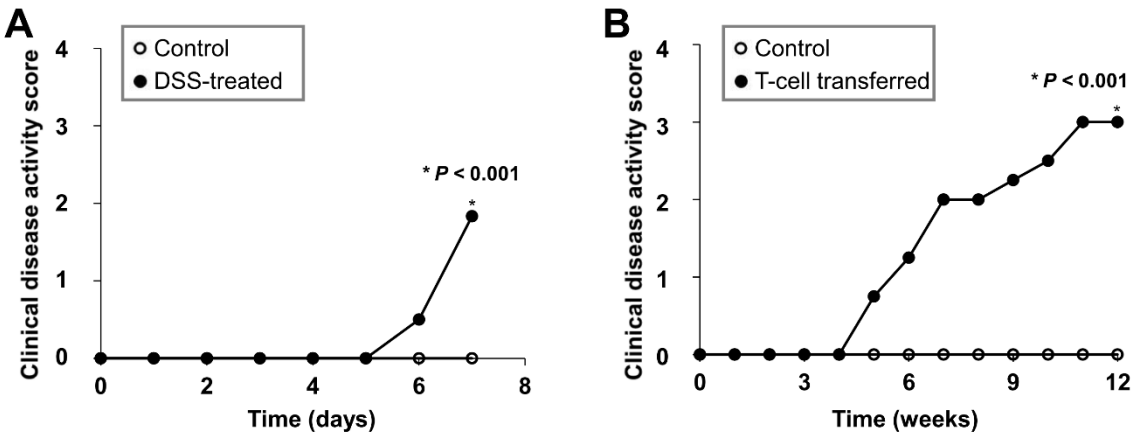

Supplemental Figure 1. Median clinical disease activity scores of mouse models of IBD induced by (A) DSS treatment and (B) adoptive transfer of T cells, as well as their respective controls.

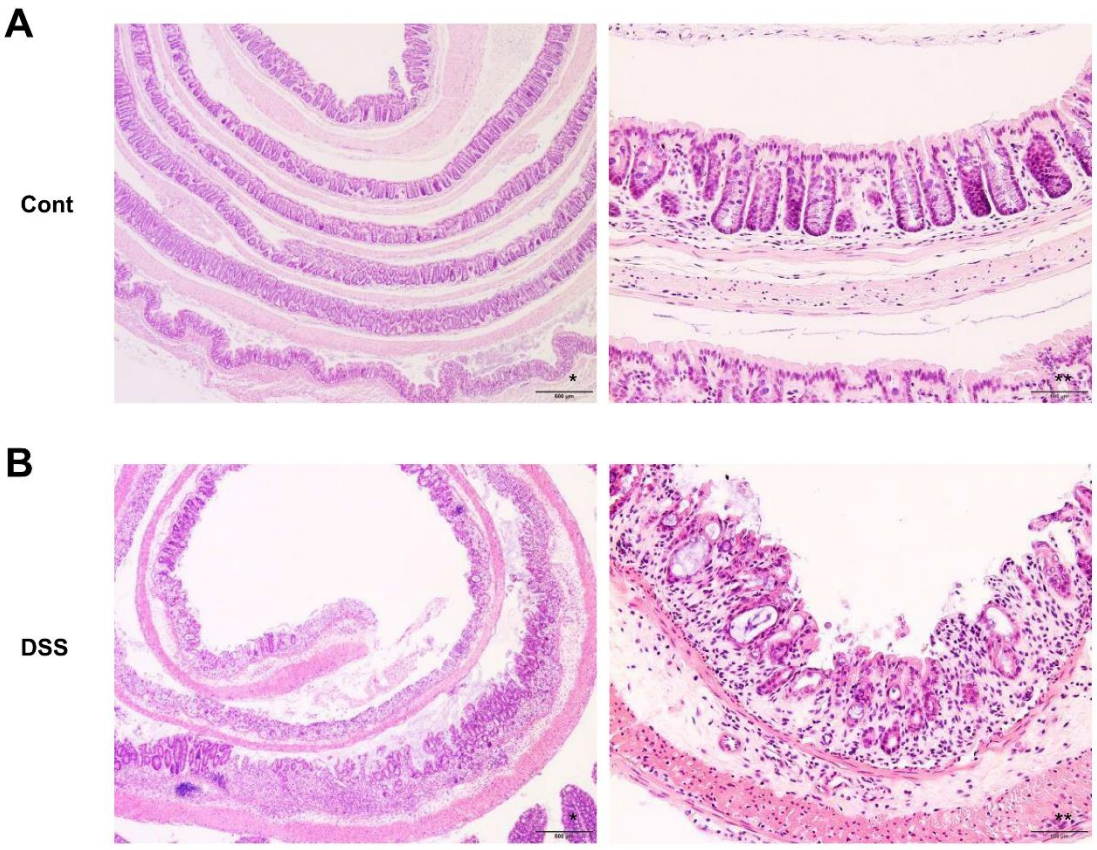

Supplemental Figure 2. Representative images of hematoxylin–eosin-stained colonic sections of (A) normal control and (B) DSS-treated Balb/c mice. Colon epithelium was severely damaged and infiltrated with inflammatory cells after DSS treatment. Images were viewed using an Olympus BX-53 microscope (Olympus, Japan). Scale bar = 500 μm (*) and 100 μm (**).

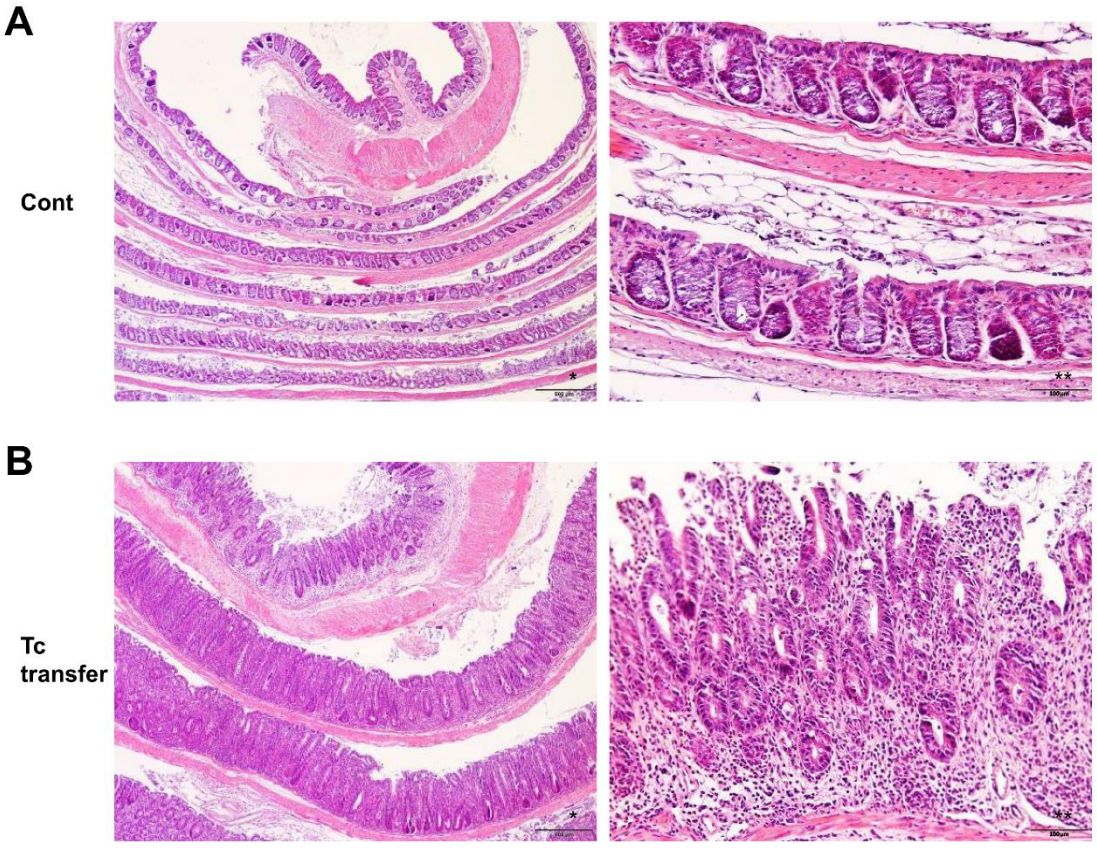

Supplemental Figure 3. Representative images of hematoxylin–eosin-stained colonic sections of (A) control and (B) adoptive T-cell–transferred BALB/c-Rag2$^{-/-}$γc$^{-/-}$ mice (B). T-cell–transferred mice exhibit markedly elongated crypts, a reduced number of goblet cells, and increased infiltration of inflammatory cells in the lamina propria. Images were viewed using an Olympus BX-53 microscope (Olympus, Japan). Scale bar = 500 μm (*) and 100 μm (**).

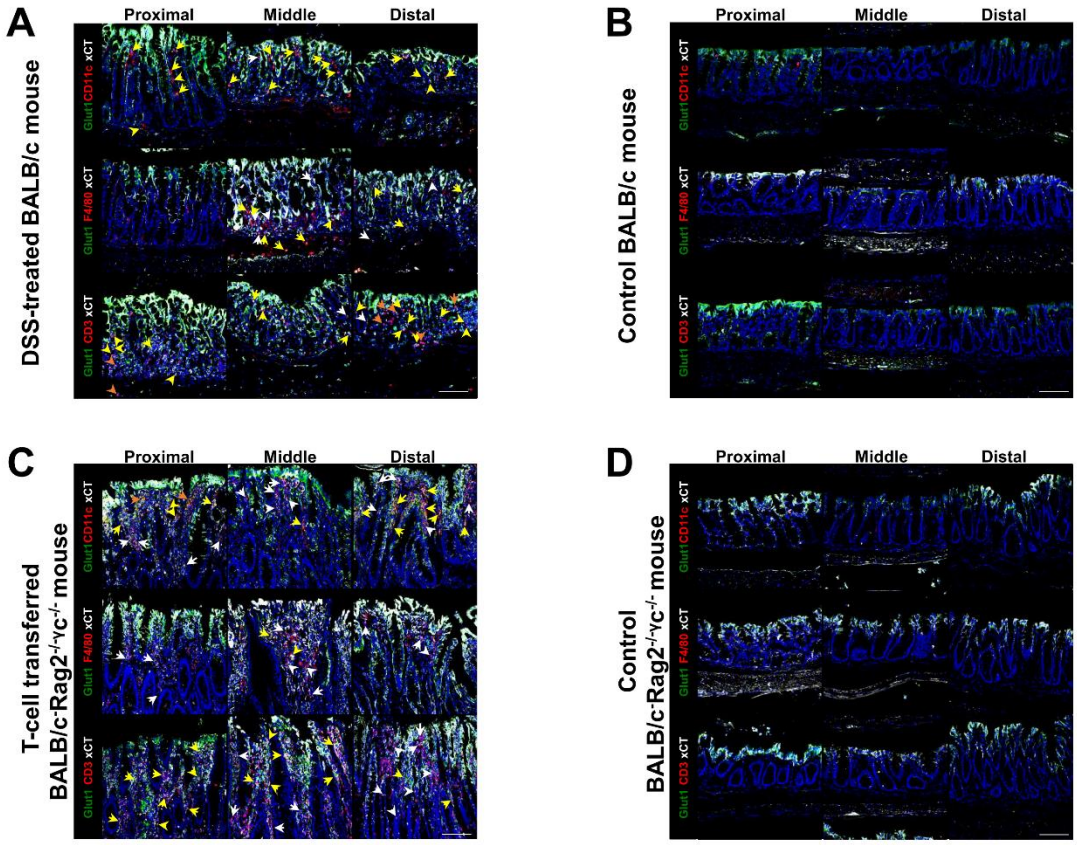

Supplemental Figure 4. Confocal microscopic images of colonic sections from experimental IBD and normal control mice. Representative xCT (white), Glut1 (green), and cell surface marker (red) immunohistochemical images of (A) DSS-treated and (B) control BalB/c mice, and of (C) adoptive T-cell–transferred and (D) control BALB/c-Rag2$^{-/-}$γc$^{-/-}$ mice. The first column shows images of the proximal colons, followed by the middle and distal colons. The intestinal epithelia of both experimental colitis and control mice were positive for xCT and Glut1 staining. However, increased numbers of xCT or Glut1 positive inflammatory cells (CD11c^{+} dendritic cells, F4/80^{+} macrophages, and CD3^{+} T cells) were observed in the lamina propria of (A) DSS-treated and (C) adoptive T-cell–transferred mice than in their respective controls. Yellow, orange, and white arrows indicate xCT/Glut1/cell surface marker-positive, Glut1/cell surface marker-positive, and xCT/cell

surface marker-positive cells, respectively. Images were viewed using an LSM 710 confocal microscope (Carl Zeiss, Oberkochen, Germany). Scale bar = 100 μm.

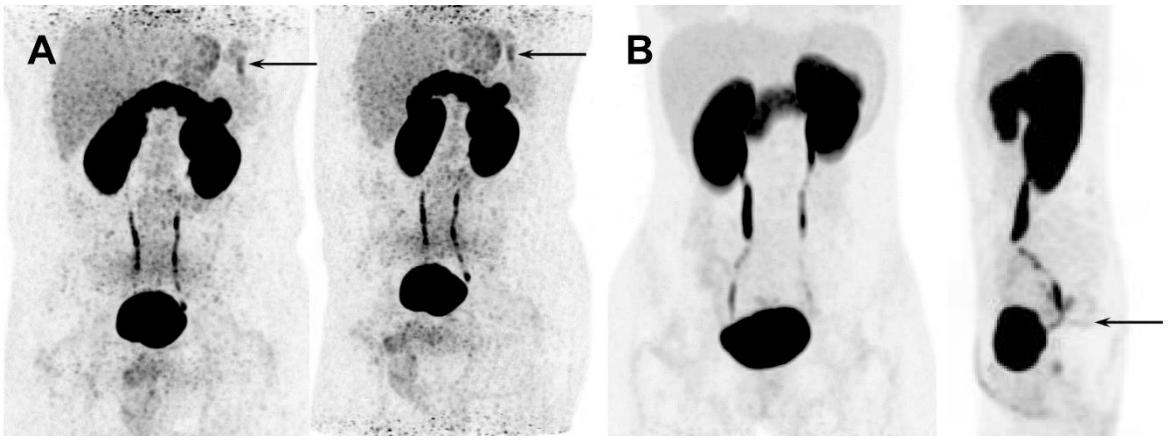

Supplemental Figure 5. False-negative ^{18}F-FSPG PET maximum intensity projection images of patients with UC. (A) Anterior and left anterior oblique images of a 32-year-old man with UC, showing a small focus of ^{18}F-FSPG uptake along the transverse colon (arrow), which was visually graded as a score of 3. The corresponding UCEIS was 4. (B) Anterior and lateral images of a 22-year-old woman with UC, showing mild ^{18}F-FSPG uptake in the rectum (arrow), which was visually interpreted as a score of 3. The corresponding UCEIS was 2.

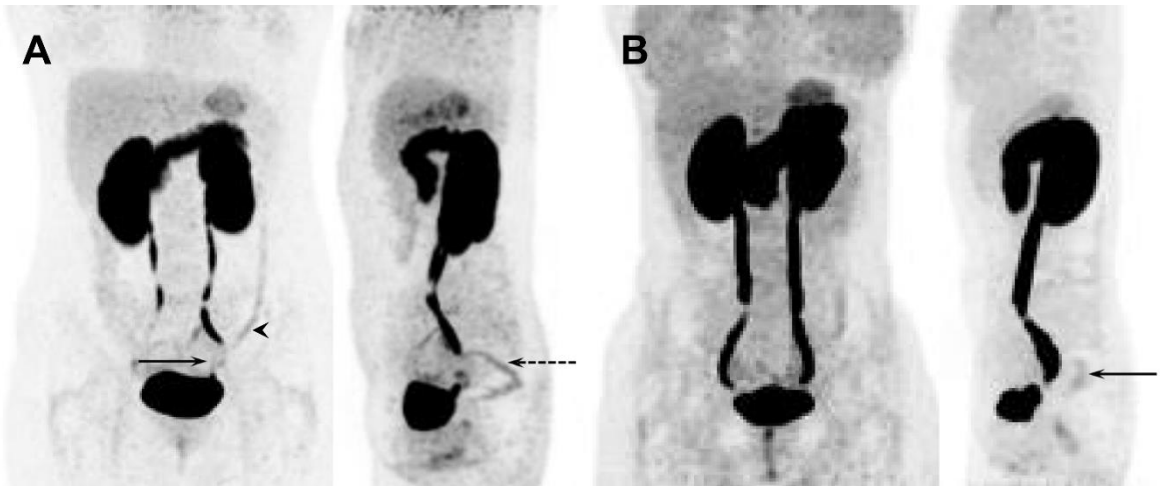

Supplemental Figure 6. False-positive ^{18}F-FSPG PET maximum intensity projection images of patients with UC. (A) Anterior and lateral images of a 41-year-old woman with UC, showing mild ^{18}F-FSPG uptake along the descending colon (arrowhead), the sigmoid colon (arrow), and the rectum (dotted arrow), all of which were visually interpreted as moderately increased intensity compared with the liver (score 4). The UCEIS was 0. (B) Anterior and lateral images of a 24-year-old woman with UC, showing mild ^{18}F-FSPG uptake in the rectum (arrow), which was also visually assessed as moderately increased intensity compared with the liver (score 4). The corresponding UCEIS was 0.

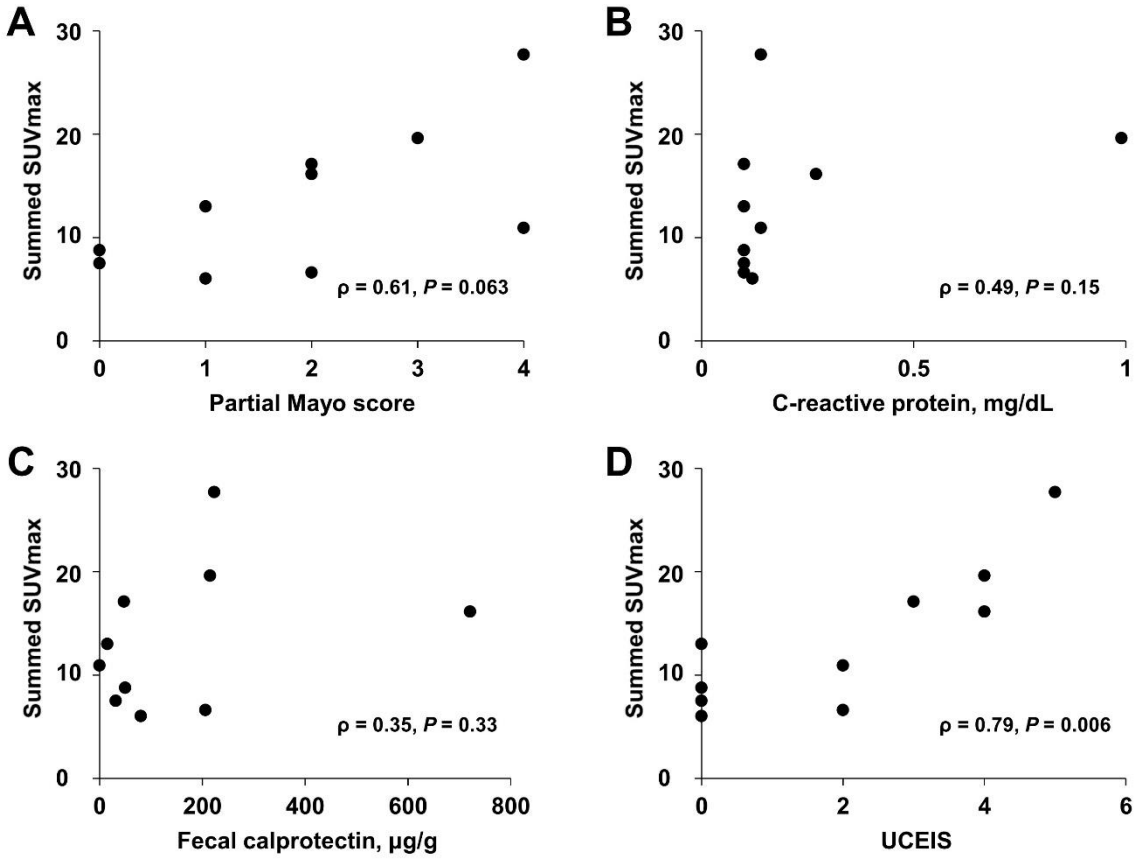

Supplemental Figure 7. Association between ^{18}F-FSPG SUVmax and markers of disease activity in patients with UC (n = 10).

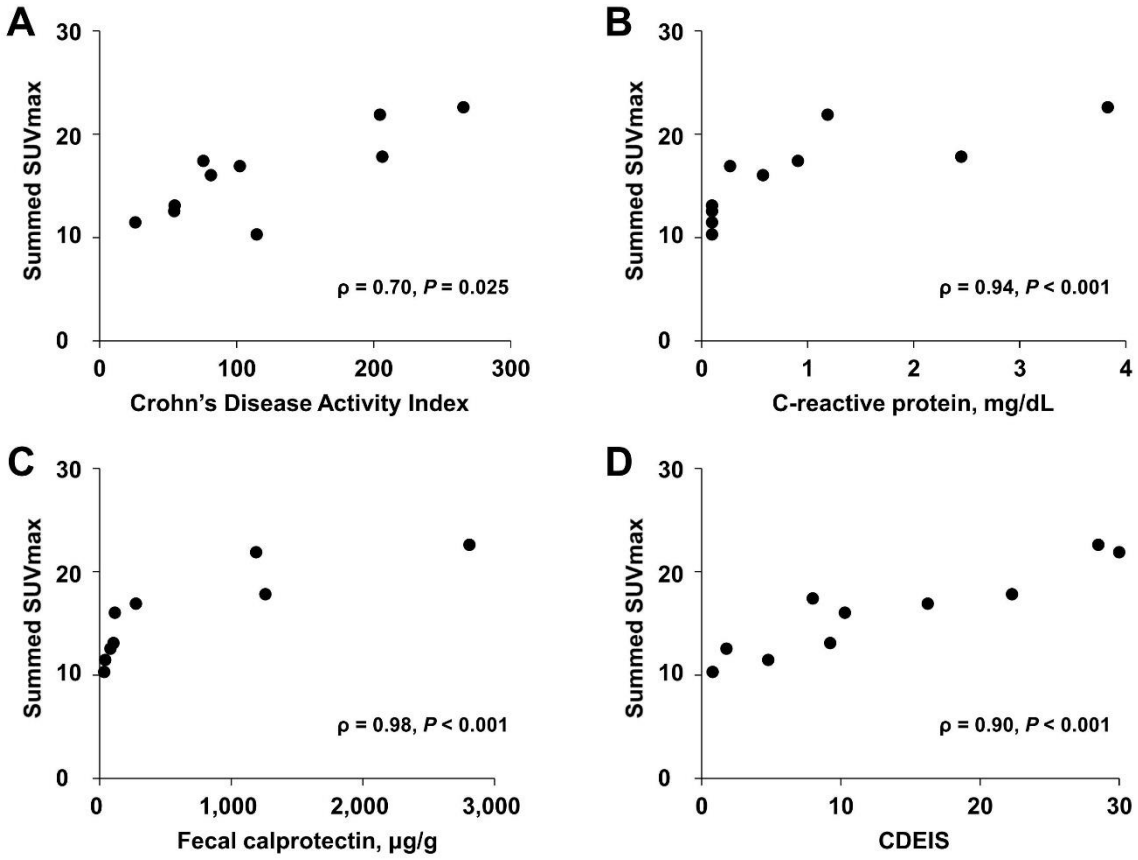

Supplemental Figure 8. Association between 18F-FSPG SUVmax and markers of disease activity in patients with CD (n = 10).

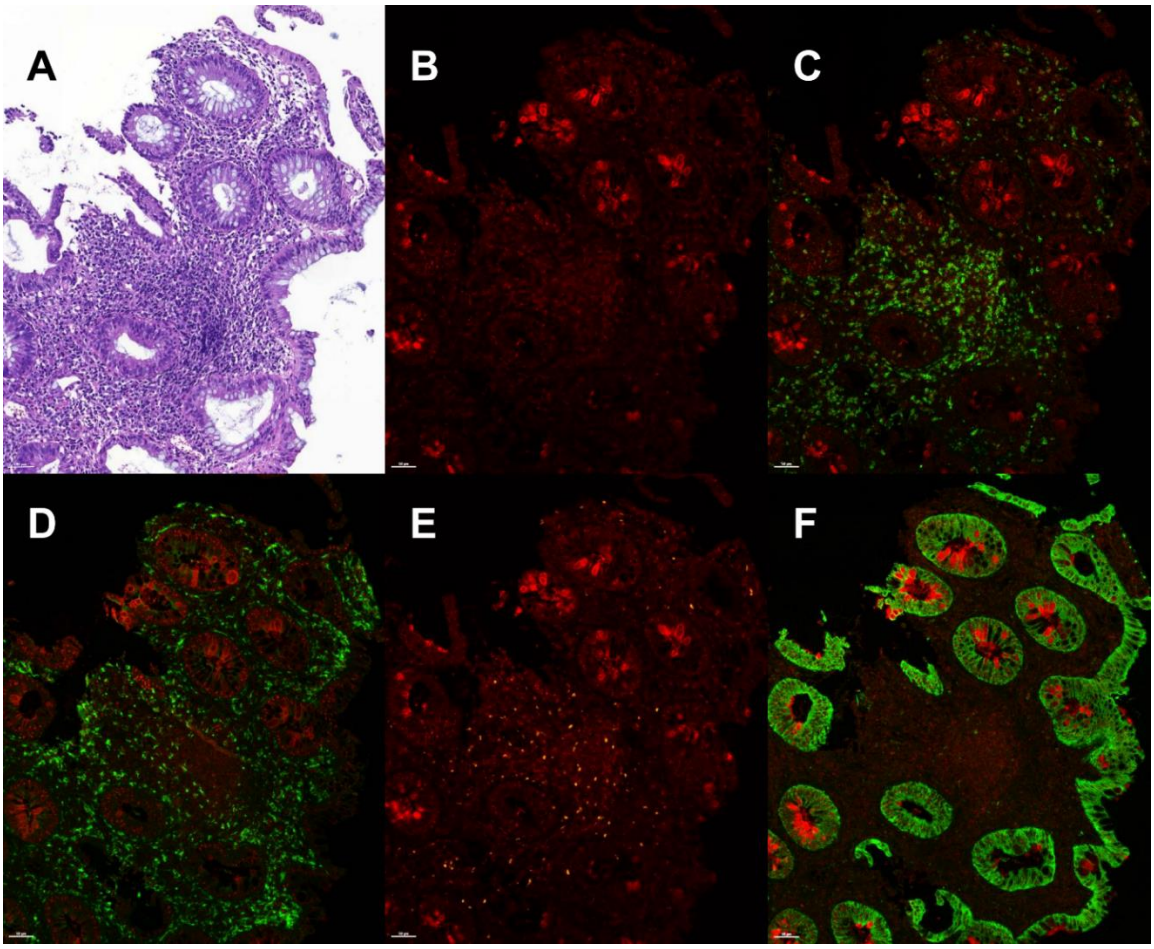

Supplemental Figure 9. Immunohistochemical staining for xCT and cell surface markers in patients with active UC. (A) Hematoxylin–eosin-stained colonic tissue and (B) immunohistochemical staining showing positive xCT expression in the epithelium and lamina propria. (C-E) Coexpression of xCT and the cell surface markers (C) CD68, (D) CD3, and (E) CD66b in the lamina propria. (F) Expression of xCT in cytokeratin-positive epithelial cells is limited to the luminal aspect of the mucosa. Color correspondence: Red = xCT; Orange = CD66b; Green = CD68, CD3, or cytokeratin. Slides were digitized using a Panoramic SCAN digital slide scanner (3 DHISTECH, Budapest, Hungary).

Scale bar = 50 μm.

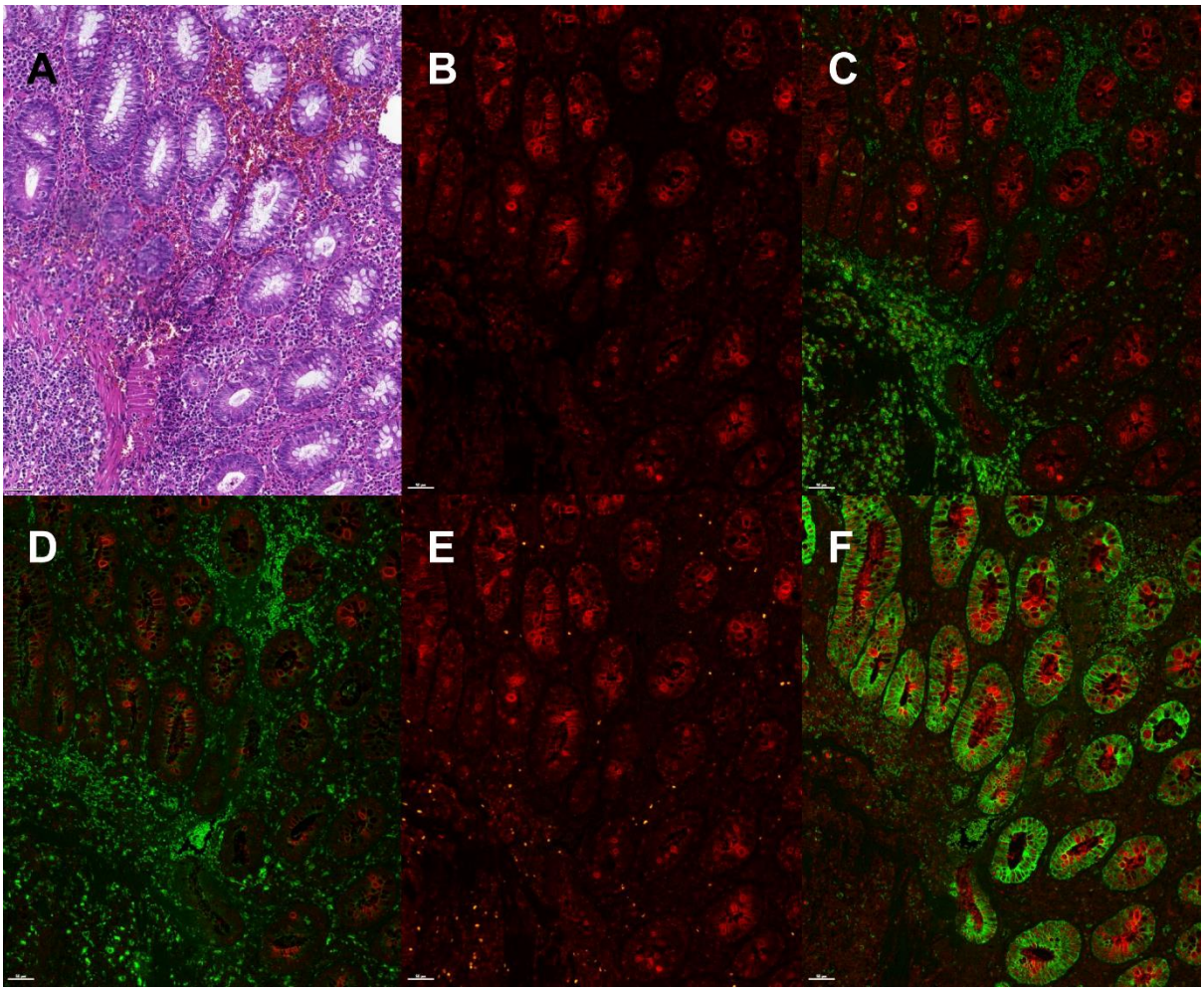

Supplemental Figure 10. Immunohistochemical staining for xCT and cell surface markers in patients with active CD. (A) Hematoxylin–eosin-stained colonic tissue and (B) immunohistochemical staining show positive xCT expression in the epithelium and lamina propria. (C-E) Coexpression of xCT and the cell surface markers (C) CD68, (D) CD3, and (E) CD6bb in the lamina propria. (F) Expression of xCT in cytokeratin-positive epithelial cells is limited to the luminal aspect of the mucosa. Color correspondence: Red = xCT; Orange = CD66b; Green = CD68, CD3, or cytokeratin. Scale bar = 50 μm.

Supplemental Table 1. List of primary antibodies used for immunohistochemical staining of xCT and cell surface markers.

[a]Primary antibody	Clone (Supplier)	Antibody titer
xCT	Polyclonal (NB300-318, Novus Biologicals)	1:250
GLUT1	Polyclonal (ab15309, Abcam)	1:200
CD68	PG-M1 (M0876, Dako Products, Agilent)	1:100
CD3	2GV6 (790-4341, Ventana)	1:200
CD66b	G10F5 (NB100-77808, Novus Biologicals)	1:500
Cytokeratin	AE-1/AE-3 (NBP2-29429, Novus Biologicals)	1:300

[a]Tyrimide signal amplification: Opal 520 for CD68, CD3, and cytokeratin; Opal 620 for CD66b; Opal 650 and 690 for xCT; Opal 780 for GLUT1.

Supplemental Table 2. Validity of ^{18}F-FSPG PET/CT for diagnosis of active ulcerative colitis.

	Patients with active ulcerative colitis		
^{18}F-FSPG PET/CT	**Positive**	**Negative**	**Total**
Positive	4	2	6
Negative	2	2	4
Total	6	4	10
	Bowel segments with active ulcerative colitis		
^{18}F-FSPG PET/CT	**Positive**	**Negative**	**Total**
Positive	9	5	14
Negative	3	30	33
Total	12	35	47

Supplemental Table 3. Validity of ^{18}F-FSPG PET/CT for diagnosis of active Crohn's disease.

	Patients with active Crohn's disease		
^{18}F-FSPG PET/CT	**Positive**	**Negative**	**Total**
Positive	8	0	8
Negative	0	2	2
Total	8	2	10
	Bowel segments with active Crohn's disease		
^{18}F-FSPG PET/CT	**Positive**	**Negative**	**Total**
Positive	17	1	18
Negative	7	16	23
Total	24	17	41

Supplemental Table 4. Immunohistochemical determination of the expression of xCT and cell surface markers and their association with UCEIS and quantitative ^{18}F-FSPG uptake in 22 bowel segments in patients with UC.

Immunohistochemistry		**Cell number / mm^2**		**UCEIS**		**SUV**	
Cell	**xCT**	**Median**	**Range**	**ρ**	***P*-value**	**ρ**	***P*-value**
CD68+	xCT$^+$	153	9–594	0.54	0.010	0.57	0.006
	xCT$^-$	51	5–309	0.33	0.129	0.29	0.191
	GLUT1$^+$	5	0–183	0.30	0.183	0.13	0.567
CD3+	xCT$^+$	281	30–8705	0.70	<0.001	0.69	<0.001
	xCT$^-$	521	58–1480	0.17	0.442	0.22	0.334
	GLUT1$^+$	37	0–814	0.16	0.477	0.07	0.747
CD66b+	xCT$^+$	93	0–1532	0.35	0.111	0.43	0.048
	xCT$^-$	67	0–2544	0.59	0.004	0.67	0.001
	GLUT1$^+$	17	0–429	0.22	0.330	0.24	0.290
CK+	xCT$^+$	2430	308–4103	–0.63	0.002	–0.61	0.002
	xCT$^-$	142	52–1067	−0.00	0.993	−0.05	0.832
	GLUT1$^+$	0	0–71	0.06	0.794	−0.05	0.829

Supplemental Table 5. Immunohistochemical determination of the expression of xCT and cell surface markers and their association with CDEIS and quantitative ^{18}F-FSPG uptake in seven bowel segments in patients with CD.

Immunohistochemistry		**Cell number / mm^2**		**CDEIS**		**SUVmax**	
Cell	**xCT**	**Median**	**Range**	**ρ**	***P*-value**	**ρ**	***P*-value**
CD68+	xCT$^+$	111	24–541	0.95	0.001	0.21	0.645
	xCT$^-$	121	46–298	−0.44	0.328	0.07	0.879
	GLUT1$^+$	10	0–25	0.18	0.694	0.14	0.758
CD3+	xCT$^+$	570	153–1229	0.35	0.448	0.46	0.294
	xCT$^-$	414	47–1428	0.06	0.908	0.54	0.215
	GLUT1$^+$	14	6–52	0.66	0.111	−0.21	0.645
CD66b+	xCT$^+$	50	0–852	0.68	0.093	0.22	0.632
	xCT$^-$	311	0–736	0.13	0.786	−0.11	0.819
	GLUT1$^+$	43	0–201	0.16	0.738	−0.02	0.969
CK+	xCT$^+$	2992	2447–4769	0.20	0.667	0.54	0.215
	xCT$^-$	596	249-1335	−0.49	0.263	0.11	0.819
	GLUT1$^+$	6	0–164	−0.27	0.564	0.13	0.788

Supplemental References

1. Baek S, Mueller A, Lim YS, et al. (4S)-4-(3-18F-fluoropropyl)-L-glutamate for imaging of xC transporter activity in hepatocellular carcinoma using PET: preclinical and exploratory clinical studies. *J Nucl Med.* 2013;54:117-123.

2. Chae SY, Choi CM, Shim TS, et al. Exploratory clinical investigation of (4S)-4-(3-18F-fluoropropyl)-L-glutamate PET of inflammatory and infectious lesions. *J Nucl Med.* 2016;57:67-69.

3. Walsh AJ, Bryant RV, Travis SP. Current best practice for disease activity assessment in IBD. *Nat Rev Gastroenterol Hepatol.* 2016;13:567-579.

4. Ahn J, Jin M, Song E, et al. Immune profiling of advanced thyroid cancers using fluorescent multiplex immunohistochemistry. *Thyroid.* 2021;31:61-67.